

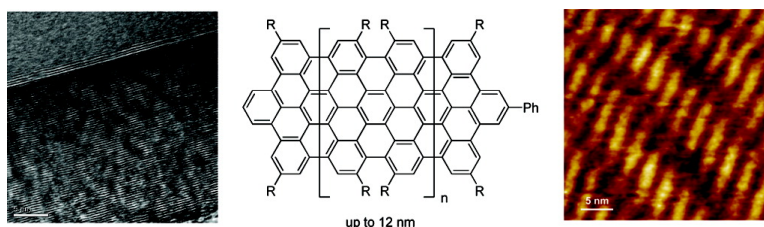
Communication

Two-Dimensional Graphene Nanoribbons

Xiaoyin Yang, Xi Dou, Ali Rouhanipour, Linjie Zhi, Hans Joachim Roder, and Klaus Müllen

J. Am. Chem. Soc., **2008**, 130 (13), 4216-4217 • DOI: 10.1021/ja710234t

Downloaded from <http://pubs.acs.org> on December 19, 2008



More About This Article

Additional resources and features associated with this article are available within the HTML version:

- Supporting Information
- Links to the 2 articles that cite this article, as of the time of this article download
- Access to high resolution figures
- Links to articles and content related to this article
- Copyright permission to reproduce figures and/or text from this article

[View the Full Text HTML](#)



ACS Publications
High quality. High impact.

Two-Dimensional Graphene Nanoribbons

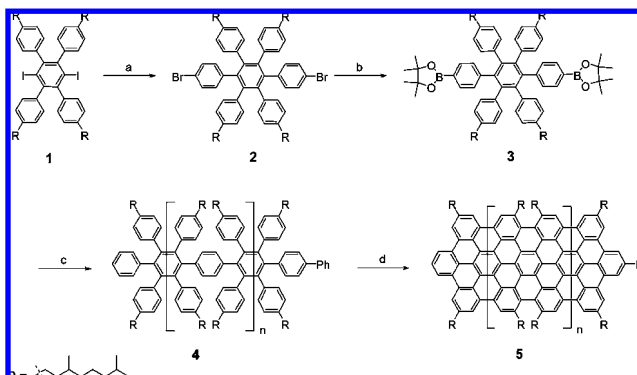
Xiaoyin Yang, Xi Dou, Ali Rouhanipour, Linjie Zhi, Hans Joachim Räder, and Klaus Müllen*

Max-Planck-Institute for Polymer Research, Ackermannweg 10, D-55128 Mainz, Germany

Received November 12, 2007; E-mail: muellen@mpip-mainz.mpg.de

Graphene nanoribbons have recently attracted attention because they are recognized as promising building blocks for nanoelectronic and spintronic devices in the carbon family.¹ The interest in this material has grown exponentially after free-standing graphenes were unexpectedly found 3 years ago and follow-up experiments confirmed their massless Dirac fermion charge carrier abilities.² Several methods have been reported to produce graphene sheets based on exfoliation or chemical oxidation of graphite or heat treatment of silicon carbide.³ However, the uncontrollable character of these methods or in some case the harsh conditions strongly restrict the quality of the resulting graphenes and consequently limit their applications. Organic synthetic protocols leading to graphene-type molecules with different size have been well developed by us and others;⁴ however, with increasing molecular size, the synthesis faced problems due to the limited solubility and the occurrence of side reactions.⁵ Herein, we describe a novel method for the synthesis of linear two-dimensional graphene nanoribbons with lengths of up to 12 nm which was never achieved before by a bottom up approach. The nanoribbons are characterized by mass spectrometry (MS), UV/vis, scanning electron microscopy (SEM), transmission electron microscopy (TEM), and scanning tunneling microscopy (STM).

The overall synthetic strategy toward these two-dimensional graphene nanoribbons is outlined in Scheme 1. The Suzuki-Miyaura coupling of 1,4-diiodo-2,3,5,6-tetraphenylbenzene **1** with 4-bromophenylboronic acid under our recently developed reaction conditions for 24 h gave hexaphenylbenzene derivative **2** in 93% yield.⁶ Twofold lithiation of compound **2** with *n*-butyllithium in THF at $-78\text{ }^{\circ}\text{C}$ for 1 h, followed by reaction with 2-isopropoxy-4,4,5,5-tetramethyl-[1,3,2]dioxaborolane, led to the *bis*-boronic ester **3** in 82% yield.⁷ Remarkably, the Suzuki-Miyaura polymerization of compound **3** with diiodobenzene **1** at $120\text{ }^{\circ}\text{C}$ (3 d) successfully furnished the polyphenylenes **4** in 75% yield. To the best of our knowledge, such a strongly sterically hindered Suzuki-Miyaura polymerization has never been reported before, and our method provides a unique access to highly crowded polyaromatics.⁸ Gel-permeation chromatography (GPC) analysis with polystyrene (PS) standard indicated a number-average molecular weight of $M_n = 1.39 \times 10^4\text{ g} \times \text{mol}^{-1}$ with a low polydispersity value of $\text{PD} = 1.2$. This unusually low polydispersity of polymer **4** is due to some fractionation by filtration of the THF solution. The low PD value of **4** is also supported by matrix-assisted laser desorption/ionization time-of-flight (MALDI-TOF) mass spectrometry (MS) showing a narrow molecular weight distribution with signals between $m/z = 6000$ and $16\,000$. While the MS clearly supports the structure by showing a signal pattern typical for the A-B type polymerization, a more detailed analysis also requires consideration of the outcome of the quenching reactions with bromobenzene and phenylboronic acid after polymerization, respectively (see the Supporting Information). Intramolecular Scholl reaction of the soluble part of **4** with FeCl_3 as oxidative reagent at room temperature (2 d) provided polymer **5** as a black solid in 65% yield.⁹ It is noteworthy that

Scheme 1. Synthesis of Graphene Nanoribbon **5**^a

^a Reagents and conditions: (a) 4-bromophenylboronic acid, $\text{Pd}(\text{PPh}_3)_4$, aliquat 336, K_2CO_3 , toluene, $80\text{ }^{\circ}\text{C}$, 24 h, 93%. (b) (i) *n*-BuLi, THF, $-78\text{ }^{\circ}\text{C}$, 1 h; (ii) 2-isopropoxy-4,4,5,5-tetramethyl-[1,3,2]dioxaborolane, rt, 2 h, 82%. (c) compound **1**, $\text{Pd}(\text{PPh}_3)_4$, aliquat 336, K_2CO_3 , toluene/ H_2O , reflux, 72 h, 75%. (d) FeCl_3 , $\text{CH}_2\text{Cl}_2/\text{CH}_3\text{NO}_2$, $25\text{ }^{\circ}\text{C}$, 48 h, 65%.

Table 1. Cyclodehydrogenation Efficiency

n^c	6	7	8	9	10	11	12
$N_{\text{H}}(\text{T.})$	88	108	120	140	152	172	184
$N_{\text{H}}(\text{R.})^b$	79	94	111	134	146	171	176
$N_{\text{H}}(\text{T.})/N_{\text{H}}(\text{R.})$	90%	87%	93%	96%	96%	99%	96%

^a $N_{\text{H}}(\text{T.})$: theoretical number of lost protons during cyclodehydrogenation.

^b $N_{\text{H}}(\text{R.})$: number of lost protons derived from MALDI-TOF measurement of polymers **4** and **5**. ^c n : number of repeat units.

polymer **5** dissolves well in common organic solvents, such as THF and dichloromethane. The good solubility can be attributed to the introduction of a large number of branched alkyl chains at adjacent positions of the aromatic periphery, which are known to reduce aggregation in solution.

The comparison of the MALDI-TOF spectra of polymers **4** and **5** clearly demonstrated that the Scholl reaction of polymer **4** proceeded very well, since the signal pattern as well as the molecular weight distribution of **5** is nearly identical to that of polymer **4** (see the Supporting Information), however, with a significant decrease in the molecular weight of the repeat units due to the loss of hydrogens during the cyclodehydrogenation reaction. The yield of the dehydrogenation step can be calculated by the mass difference of the theoretical molecular weight and the experimental molecular weight as obtained by MS corresponding to the hydrogen loss during the reaction. The results for the different number of repeat units (Table 1) reveal an almost complete conversion with an average number of 94%. This is a strong “chemical” support for the formation of the graphene nanoribbons.

The UV spectrum of **5** ($\lambda_{\text{max}} = 485\text{ nm}$, recorded in THF) showed a significant red shift of about 200 nm comparing to the absorption of the precursor polymer **4** (see the Supporting Information). The maximum absorption of **5** also exhibits a significant bathochromic shift with respect to the smaller reference compounds **6** ($\lambda_{\text{max}} =$

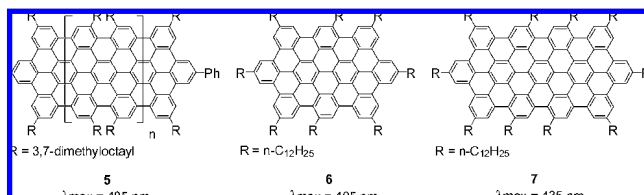


Figure 1. Maximum absorption of graphene **5**, compounds **6** and **7**.

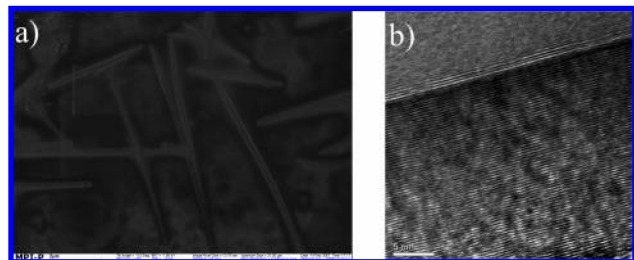


Figure 2. The SEM and TEM images of polymer **5**.

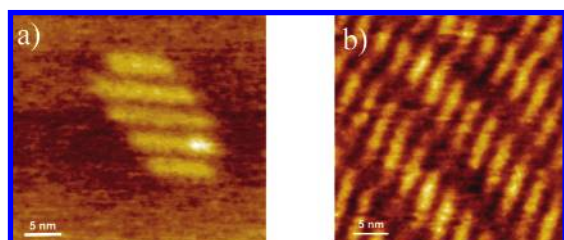


Figure 3. The STM images of **5** at the solid/liquid interface on HOPG.

405 nm) and **7** ($\lambda_{\text{max}} = 435$ nm) (Figure 1)¹⁰ even being probably more nonplanar because of the sterical hindrance of two side chains in the same bay region. These spectroscopic results further confirmed that the FeCl_3 mediated intramolecular oxidative cyclo-dehydrogenation of polymer **4** indeed gave rise to the extended aromatic system **5**.

Drop-casting of the THF solution of **5** onto a silica substrate produced one-dimensional nanoscale objects with a diameter of about 100 nm and a length of up to 5 μm in SEM measurement, suggesting a high tendency of the nanographenes to crystallize in the solid state (Figure 2a).¹¹ TEM characterization of these objects further disclosed a well-ordered stacking of the graphene layers (Figure 2b). The d-spacing of the lattice was calculated as 3.4 Å, in agreement with the typical distance of π - π stacking of the nanographenes.¹²

A powerful method to investigate the two-dimensional organization of organic molecules by physisorption on surfaces is STM at the solid–liquid interface, which provides information on structure and dynamics on the single-molecular level.¹³ As a result of the good solubility of **5**, it was possible for the first time to prepare highly ordered monolayers (2D crystal) of such larger graphene ribbons. Figure 3 shows the corresponding STM images obtained in situ at the interface between a solution of **5** in *n*-dodecane and the basal plane of highly oriented pyrolytic graphite (HOPG). Figure 3a visualizes an isolated small aggregate with an ensemble of five molecules having lengths from 8 to 12 nm. The objects are oriented parallel to each other and show an equal spacing of 2.9 nm. A similar arrangement is also found in extended layers as shown in Figure 3b where again the nanoribbons are aligned parallel to each other. They build up extended rows on the μm scale with molecules

titled by around 60° with respect to the row axis. The layer appears as an overall regular lamellar pattern despite the size distribution of the individual molecules. The length distribution of the objects as well as their uniform width and spacing fit very well to the molecular dimension of polymer **5** as obtained from molecular modeling (ca. 2.7 nm width and ca. 9.2 nm length at 10 000 g/mol) and suggest a face-on arrangement of the molecules at the surface of HOPG as commonly observed for similar molecules.¹⁴

In conclusion, a new synthetic protocol yielding novel two-dimensional graphene nanoribbons has been developed. Both UV/vis absorption spectroscopy and MALDI-TOF mass spectrometry studies revealed the formation of graphene nanoribbons. Various microscopic studies of these novel structures showed a high tendency to self-assemble. Further optoelectronic applications of our nanographenes in FETs and photovoltaic devices are currently in progress in our laboratory.

Acknowledgment. We acknowledge financial support from the European Commission Project NAIMO (NMP4-CT-2004-500355) and the Bundesministerium für Bildung und Forschung (Solar Cell Network).

Supporting Information Available: Experimental procedures, ^1H NMR, ^{13}C NMR, UV–vis spectra, MALDI-TOF spectra, SEM, TEM, and STM images. This material is available free of charge via the Internet at <http://pubs.acs.org>.

References

- (1) (a) Geim, A. K.; Novoselov, K. S. *Nat. Mater.* **2007**, *6*, 183. (b) Heersche, H. B.; Jarillo-Herrero, P.; Oostinga, J. B.; Vandersypen, L. M. K.; Morpurgo, A. F. *Nature* **2007**, *446*, 56. (c) Tsefrikas, V. M.; Scott, L. T. *Chem. Rev.* **2006**, *106*, 4868. (d) Watson, M. D.; Fechtenkötter, A.; Müllen, K. *Chem. Rev.* **2001**, *101*, 1267. (e) Vostrowsky, O.; Hirsch, A. *Chem. Rev.* **2006**, *106*, 5191. (f) Mueller, T. J. J.; Bunz, U. H. F. *Functional Organic Materials*; Wiley-VCH: Weinheim, 2007.
- (2) (a) Zhang, Y.; Tan, Y.-W.; Stromier, H. L.; Kim, P. *Nature* **2005**, *438*, 201. (b) Berger, C.; Song, Z.; Li, X.; Wu, X.; Brown, N.; Nafud, C.; Mayo, D.; Li, T.; Marchenkov, A. N.; Conrad, E. H.; First, P. N.; de Heer, W. A. *Science* **2006**, *312*, 1191. (c) Ohta, T.; Bostwick, A.; Seyller, T.; Horn, K.; Rotenberg, E. *Science* **2006**, *313*, 951.
- (3) (a) Shioyama, H. *J. Mater. Sci. Lett.* **2001**, *20*, 499. (b) Krishnan, A.; Dujardin, E.; Treacy, M. M. J.; Hugdahl, J.; Lynum, S.; Ebbesen, T. W. *Nature* **1997**, *388*, 451. (c) Dresselhaus, M. S.; Dresselhaus, G. *Adv. Phys.* **2002**, *51*, 1. (d) Viculis, L. M.; Mack, J. J.; Kaner, R. B. *Science* **2003**, *299*, 1361. (e) Land, T. A.; Michely, T.; Behm, R. J.; Hemminger, J. C.; Comsa, G. *Surf. Sci.* **1992**, *264*, 261.
- (4) (a) Scott, L. T. *Angew. Chem., Int. Ed.* **2004**, *43*, 4994. (b) Tahara, K.; Tobe, Y. *Chem. Rev.* **2006**, *106*, 5274. (c) Wu, J.; Pisula, W.; Müllen, K. *Chem. Rev.* **2007**, *107*, 718. (d) Lambert, C. *Angew. Chem., Int. Ed.* **2005**, *44*, 7337 and references therein.
- (5) Wu, J.; Gherghel, L.; Watson, M. D.; Li, J.; Wang, Z.; Simpson, C. D.; Kolb, U.; Müllen, K. *Macromolecules* **2003**, *36*, 7082.
- (6) (a) Yang, X.; Dou, X.; Müllen, K. Manuscript in preparation. (b) Dou, X.; Yang, X.; Bodwell, G. J.; Wagner, M.; Enkelmann, V.; Müllen, K. *Org. Lett.* **2007**, *9*, 2485.
- (7) Wang, F.; Bazan, G. C. *J. Am. Chem. Soc.* **2006**, *128*, 15786.
- (8) Pascal, R. A., Jr. *Chem. Rev.* **2006**, *106*, 4809.
- (9) Simpson, C. D.; Brand, J. D.; Berresheim, A. J.; Przybilla, L.; Räder, H. J.; Müllen, K. *Chem. Eur. J.* **2002**, *8*, 1424.
- (10) Iyer, V. S.; Yoshimura, K.; Enkelmann, V.; Epsch, R.; Rabe, J. P.; Müllen, K. *Angew. Chem., Int. Ed.* **1998**, *37*, 2696.
- (11) (a) Hamaoui, B. E.; Zhi, L.; Pisula, W.; Kolb, U.; Wu, J.; Müllen, K. *Chem. Commun. (Cambridge)* **2007**, 2384. (b) Wu, D.; Zhi, L.; Bodwell, G. J.; Cui, G.; Tsao, N.; Müllen, K. *Angew. Chem., Int. Ed.* **2007**, *46*, 5417.
- (12) (a) Zhi, L.; Wu, J.; Li, J.; Kolb, U.; Müllen, K. *Angew. Chem., Int. Ed.* **2005**, *44*, 2120. (b) Zhi, L.; Gorelik, T.; Wu, J.; Kolb, U.; Müllen, K. *J. Am. Chem. Soc.* **2005**, *127*, 12792.
- (13) (a) Rabe, J. P.; Buchholz, S. *Science* **1991**, *253*, 424. (b) Rabe, J. P.; Buchholz, S. *Phys. Rev. Lett.* **1991**, *66*, 2096.
- (14) Ito, S.; Wehmeier, M.; Brand, J. D.; Kubel, C.; Epsch, R.; Rabe, J. P.; Müllen, K. *Chem. Eur. J.* **2000**, *6*, 4327.

JA710234T